Analysis of Airplane Response to Nonstationary Turbulence Including Wing Bending Flexibility

YOSHINORI FUJIMORI* AND Y. K. LIN†
University of Illinois, Urbana, Ill.

Response of an airplane to atmospheric turbulence is determined analytically assuming that the turbulence field is a nonstationary random process. Specifically, the excitation field is modeled as a uniformly modulated process which is a stationary process multiplied by a deterministic envelope function. This model offers great versatility to fit different geographical peculiarities and flight missions. The airplane is idealized as a multiple-degrees-of-freedom linear system, and detail calculation is given for the plunging, pitching, and wing bending modes. The formulation follows Priestley's framework of evolutionary spectral analysis, generalized to include the evolutionary cross spectra. Numerical results are presented graphically as the mean-square frequency spectra of modal responses at different times, for both displacement and acceleration type of response.

Introduction

THE dynamic response of airplanes to atmospheric turbulence has been a major concern to aeronautical engineers especially for the design of modern flexible airplanes. Numerous studies have been documented since the 1950's assuming that the turbulence field is a stationary random process. (For a bibliography of such studies in the United States, see, for example, Ref. 1.) Only very recently has an attempt been made to consider nonstationary excitations.[2] As in most pioneering works, the analysis in Ref. 2 was restricted to the simplest case of a single degree of freedom, considering just the rigid plunging motion of a vehicle. However, other degrees of freedom must be taken into account in certain practical situations, especially for large airplanes. The present paper is devoted to the development of an analytical framework for computing multimodal response of a flight vehicle in a nonstationary turbulence field. For this purpose, the concept of evolutionary spectrum of Priestley[3] will be used and generalized to that of evolutionary cross-spectrum for the description of several nonstationary random processes. To illustrate the application of analytical results derived herein, numerical computation will be carried out for plunging, pitching and wing bending modes.

I. Evolutionary Spectral Analysis of Response of a Multidegree-of-Freedom Linear System

For a linear system, the input-output relationship may be expressed as follows:

$$\mathbf{Y} = \int_0^t [\mathbf{h}(t-\tau)]\mathbf{X}(\tau)\,d\tau \tag{1}$$

where

$\mathbf{X} = (X_1, X_2, X_3, \ldots X_n)$ = an input vector

$\mathbf{Y} = (Y_1, Y_2, Y_3, \ldots Y_n)$ = the corresponding output vector

$[\mathbf{h}]$ = matrix of impulse response functions, an $n \times n$ matrix

The components of $\mathbf{Y}$ can be written as follows

$$Y_j(t) = \sum_m \int_0^t X_m(\tau) h_{jm}(t-\tau)\,d\tau \tag{2}$$

The cross-correlation function of Y_j and Y_k is simply

$$E[Y_j(t_1)Y_k(t_2)] = \sum_m \sum_l \int_0^{t_1}\int_0^{t_2} E[X_m(\tau_1)X_l(\tau_2)] \times h_{jm}(t_1-\tau_1)h_{kl}(t_2-\tau_2)\,d\tau_1\,d\tau_2 \tag{3}$$

where $E[\ ]$ denotes an ensemble average.

We shall assume that every input component has a Stieltjes integral representation:

$$X_m(\tau) = \int_{-\infty}^{\infty} A_m(\tau,\omega)\,e^{i\omega\tau}\,d\tilde{X}_m(\omega) \tag{4}$$

where $A_m(\tau,\omega)$, $m = 1,2,\ldots,n$ are suitable deterministic functions and $\tilde{X}_m$ are complex-valued random processes with orthogonal increments; that is,

$$\begin{aligned} E[d\tilde{X}_m(\omega_1)\,d\tilde{X}_l{}^*(\omega_2)] &= 0, \quad \omega_1 \neq \omega_2 \\ E[d\tilde{X}_m(\omega)\,d\tilde{X}_l{}^*(\omega)] &= \Phi_{\tilde{X},ml}(\omega)\,d\omega \end{aligned} \tag{5}$$

where an asterisk indicates the complex conjugate. We see that every X_m is a nonstationary random process except for the special case where the A_m function reduces to a constant. Since all components of the input vector are real-valued, we may also write

$$X_l(\tau) = \int_{-\infty}^{\infty} A_l{}^*(\tau,\omega)\,e^{-i\omega\tau}\,d\tilde{X}_l{}^*(\omega) \tag{4a}$$

Then substituting Eqs. (4) and (4a) into Eq. (3), we obtain

$$E[Y_j(t_1)Y_k(t_2)] = \sum_m \sum_l \int_{-\infty}^{\infty} \left[\int_0^{t_1} A_m(\tau_1,\omega)h_{jm}(t_1-\tau_1)\,e^{i\omega\tau_1}\,d\tau_1 \times \int_0^{t_2} A_l{}^*(\tau_2,\omega)h_{kl}(t_2-\tau_2)\,e^{-i\omega\tau_2}\,d\tau_2\right]\Phi_{\tilde{X},ml}(\omega)\,d\omega \tag{6}$$

Denoting

$$M_{jm}(t,\omega) = \int_0^t A_m(t-\tau,\omega)h_{jm}(\tau)\,e^{-i\omega\tau}\,d\tau \tag{7}$$

Equation (6) can be expressed alternatively:

$$E[Y_j(t_1)Y_k(t_2)] = \sum_m \sum_l \int_{-\infty}^{\infty} e^{i\omega(t_1-t_2)}M_{jm}(t_1,\omega)M_{kl}{}^*(t_2,\omega) \times \Phi_{\tilde{X},ml}(\omega)\,d\omega \tag{8}$$

The quantity

$$\sum_m \sum_l M_{jm}(t_1,\omega)M_{kl}{}^*(t_2,\omega)\,\Phi_{\tilde{X},ml}(\omega) \tag{9}$$

will be called the evolutionary cross spectral density function

Received July 24, 1972; revision received October 10, 1972; presented as Paper 73-000 at the AIAA 11th Aerospace Sciences Meeting and Technical Display, Washington, D.C., January 10–12, 1973. The work reported herein was supported in part by National Science Foundation under Grant GK 34136X.

Index categories: Aircraft Gust Loading and Wind Shear; Aircraft Vibration; Structural Dynamic Analysis.

* Graduate student on leave from National Aerospace Laboratory, Tokyo, Japan.

† Professor of Aeronautical and Astronautical Engineering. Associate Fellow AIAA.

of the responses Y_j at time t_1 and Y_k at t_2. An evolutionary cross spectral density for two nonstationary random processes is a logical generalization of Priestley's evolutionary spectral density of a nonstationary random process.[3] When $k=j$ the right-hand side of Eq. (8) reduces to an autocorrelation function. Further letting $t_1=t_2$, Eq. (8) becomes a mean-square value, and Eq. (9) reduces to an evolutionary spectral density. Therefore, an evolutionary spectral density gives the frequency distribution of the mean-square value of a random process at a given t.

II. Application to Flight Vehicle

Consider the equations of motion of an airplane

$$M_j\ddot{\xi}_j+\beta_j\dot{\xi}_j+M_j\omega_j^2\xi_j=Q_j, \qquad j=1,2,\ldots,n \tag{10}$$

where

$M_j=\int_S\int \phi_j^2(x,y)\rho(x,y)\,dx\,dy=j$th generalized mass
$Q_j=\int_S\int\{F^M(x,y,t)+F^G(x,y,t)\}\phi_j(x,y)\,dx\,dy$
$=j$th generalized force
$F^M=$ lift per unit area due to motion of the airplane
$F^G=$ lift per unit area due to vertical gust velocity
$\xi_j=j$th generalized coordinate
$\phi_j=j$th mode
$\omega_j=j$th natural frequency
$\rho=$ mass per unit area of the airplane
$S=$ domain where ϕ_j is defined
$\beta_j=$ damping coefficient in jth mode

The functions F^M and F^G depend on the geometry and speed of the flight vehicle. In principle, they can be determined numerically, perhaps rather tediously, for every vehicle configuration and flight regime. For the purposes of the present study, however, we shall make the following approximations:

$$F^M(x,y,t)=-\pi\rho_0 b\ddot{Z}(x,y,t)/2-\pi\rho_0 U\int_0^t \ddot{Z}(x,y,t_1)\phi(t-t_1)\,dt_1 \tag{11}$$

$$F^G(x,y,t)=\pi\rho_0 U\int_0^t W(x-Ut_1,y)\dot{\psi}(t-t_1)\,dt_1 \tag{12}$$

where

$Z(x,y,t)=\sum_j \phi_j(x,y)\xi_j(t)=$ total response
$\phi(t)=$ Wagner's function
$\psi(t)=$ Küssner's function
$b=$ one-half of the reference chord length
$U=$ the airplane forward velocity
$W(x-Ut,y)=$ vertical gust velocity
$\rho_0=$ air density

As is customary, x and y are body coordinates whose origin is the gravity center of the entire airplane, which is assumed to fly in the negative direction of the x axis with a constant forward speed U. The dependence of the gust velocity W on $x-Ut$ implies that we have assumed a "frozen" turbulence field, a reasonable assumption for flight vehicle response analysis. When the chord length has a span-wise variation, we may choose a suitable reference chord $2b$ representative of the aerodynamic characteristics of the wing.

It is of interest to comment on the physical implication of the approximate expressions (11) and (12). Equation (11) gives the lift change due to the disturbed motion of the airplane. Equation (12) represents the lift change due to a vertical gust W, if the airplane were to remain at the steady forward flight. These are assumed to depend only on the local motion and local gust velocity,‡ and they are taken to be of the same forms as those for a two-dimensional incompressible flow.[4] For the Wagner and Küssner functions, appearing in Eqs. (11) and (12), we shall use the approximation[4]

$$\phi(s)=1-0.165\,e^{-0.0455s}-0.355\,e^{-0.3s}$$
$$\psi(s)=1-0.5\,e^{-0.13s}-0.5\,e^{-s}$$

‡ In a more refined analysis the lift change at a particular point (x,y) would depend on the flow over the entire airfoil.

where $s=Ut/b$. No claim is made of the accuracy when Eqs. (11) and (12) are applied to a practical airplane geometry, but they appear to be reasonable assumptions for the present study.

Using Eqs. (11) and (12) to compute the generalized force $Q_j=Q_{M,j}+Q_{G,j}$, we obtain

$$Q_{M,j}(t)=-\pi\rho_0 U\sum_m \Delta_{jm}\left[\int_0^t \ddot{\xi}_m(t_1)\phi(t-t_1)\,dt_1+\frac{b}{2U}\ddot{\xi}_m(t)\right] \tag{13}$$

$$Q_{G,j}(t)=\pi\rho_0 U\int_0^t \dot{\psi}(t-t_1)\,dt_1\int_S\int W(x-Ut_1,y)\phi_j(x,y)\,dx\,dy \tag{14}$$

where

$$\Delta_{jm}=\int_S\int \phi_j(x,y)\phi_m(x,y)\,dx\,dy$$

Now, Laplace transform of Eq. (10) yields

$$M_j p^2\bar{\xi}_j(p)+\beta_j p\bar{\xi}_j(p)+M_j\omega_j^2\bar{\xi}_j(p)+\pi\rho_0 U\sum_m \Delta_{jm}\left[p^2\bar{\phi}(p)\bar{\xi}_m(p)+\frac{b}{2U}p^2\bar{\xi}_m(p)\right]=\bar{Q}_{G,j}(p) \qquad j=1,2,\ldots,n \tag{15}$$

where the terms related to $Q_{M,j}$ have been moved to the left-hand side. It is seen from Eq. (15) that motion of the jth mode is coupled with that of other modes; therefore, we must solve the matrix equation

$$[C_{jm}]\{\bar{\xi}_j(p)\}=\{\bar{Q}_{G,j}\} \tag{16}$$

The solution of Eq. (16) is given by

$$\bar{\xi}_j(p)=\sum_m a_{jm}|C_{jm}|^{-1}\,\bar{Q}_{G,m}(p) \tag{17}$$

where $|C_{jm}|=$ the determinant of matrix $[C_{jm}]$ and $a_{jm}=$ the cofactor of element c_{jm}.

Taking the inverse Laplace transform of Eq. (17), we have

$$\xi_j(t)=\sum_m\int_0^t h_{jm}(t-\tau)Q_{G,m}(\tau)\,d\tau \tag{18}$$

where

$$h_{jm}(u)=\mathscr{L}^{-1}(a_{jm}|C_{jm}|^{-1})$$

Comparing Eqs. (2) and (18), we see that $Q_{G,m}$ plays the role of the input X_m and ξ_j the role of the output Y_j. Thus, using Eqs. (3) and (14) we obtain

$$E[\xi_j(t_1)\xi_k(t_2)]=(\pi\rho_0 U)^2\sum_m\sum_l\int_0^{t_1}h_{jm}(t_1-\tau_1)\,d\tau_1\times\int_0^{t_2}h_{kl}(t_2-\tau_2)\,d\tau_2\int_0^{\tau_1}\dot{\psi}(\tau_1-\sigma_1)\,d\sigma_1\int_0^{\tau_2}\dot{\psi}(\tau_2-\sigma_2)\,d\sigma_2\times\int_S\int_S\int_S\int E[W(x_1-U\sigma_1,y_1)W(x_2-U\sigma_2,y_2)]\phi_m(x_1,y_1)\times\phi_l(x_2,y_2)\,dx_2\,dy_2\,dx_1\,dy_1 \tag{19}$$

Although the gust velocity W is a nonstationary random process, we shall assume that it can be factored into the following product:

$$W(x-Ut,y)=C(x-Ut,y)G(x-Ut,y) \tag{20}$$

where $C(x-Ut,y)=$ a deterministic envelope function and $G(x-Ut,y)=$ a stationary random process. A nonstationary random process having the above representation is called a uniformly modulated process,[3] the nonstationarity being the result of amplitude modulation. We shall assume that the stationary factor G of the gust has a cross-spectral density function $\Phi(\omega,\xi,\eta)$ as follows:

$$\Phi(\omega,\xi,\eta)=2(\pi U)^{-1}\sigma_G^2 L_G\exp(-i\omega\xi/U)\{(4a^2)^{-1}(\omega/U)^2\eta^2\times K_2(a\eta/L_G)+(2a)^{-2}(a\eta/L_G)[3K_1(a\eta/L_G)-(a\eta/L_G)\times K_2(a\eta/L_G)]\} \tag{21}$$

where

$$\xi=x_1-x_2, \qquad \eta=y_1-y_2$$

$\sigma_G=$ root mean square value of $G(x-Ut,y)$, $L_G=$ turbulence

scale of G, $a=[1+(L_G\omega/U)^2]^{1/2}$, and K_1 and K_2 = modified Bessel functions of the second kind. This cross spectral density is related to the correlation function of G by

$$E[G(x_1-Ut_1,y_1)G(x_2-Ut_2,y_2)]=\int_{-\infty}^{\infty}\Phi(\omega,\xi,\eta)\,e^{i\omega(t_1-t_2)}\,d\omega \qquad (22)$$

Equation (21) was obtained by Lin[5] for a homogeneous and isotropic gust field.

A uniformly modulated process, such as the one given in Eq. (20), admits the Stieltjes integral representation of the type of Eq. (4). In particular,

$$W(x-Ut,y)=\int_{-\infty}^{\infty}C(x-Ut,y)\,e^{i\omega t}\,d\tilde{G}(\omega,x,y) \qquad (23)$$

It can be shown by using Eqs. (20) and (22) that

$$\begin{aligned}E[d\tilde{G}(\omega_1,x_1,y_1)\,d\tilde{G}^*(\omega_2,x_2,y_2)]&=0, \quad \omega_1\neq\omega_2\\ E[d\tilde{G}(\omega,x_1,y_1)\,d\tilde{G}^*(\omega_2,x_2,y_2)]&=\Phi(\omega,\xi,\eta)\,d\omega\end{aligned} \qquad (24)$$

Therefore, $C(x-Ut,y)$ in Eq. (23), although independent of ω, plays the role of $A_m(t,\omega)$ in Eq. (4), and $\Phi(\omega,\xi,\eta)$ the role of $\Phi_{\tilde{\chi},ml}(\omega)$.

For most applications, the envelope function of a uniformly modulated process is a slowly varying function of its argument (or arguments). For the present study, we shall choose a versatile form as follows:

$$C(x-Ut,y)=C_0[e^{\alpha(x-Ut)}-e^{\beta(x-Ut)}]1(Ut-x) \qquad (25)$$

where C_0 = normalizing constant, α,β = arbitrary constants, and $0\leqq\alpha<\beta$

$$\begin{aligned}1(Ut-x)&=0 \quad \text{for} \quad Ut-x<0\\ &=1 \qquad\quad Ut-x>0\end{aligned}$$

This form of envelope function has been used in the previous investigation where only the rigid plunging motion was considered.[2] It was also used by Shinozuka[6] to characterize earthquake excitations. As is implied in Eq. (25), the nonstationarity of the process in the y direction has been neglected. This is a reasonable simplification since the change of statistical property of a gust field over a distance of the order of the normal size of an airplane should be quite small.

Introducing, for convenience, the following new notations:

$$\Theta_{ml,\alpha\beta}(\omega)=\int_S\int_S\Phi(\omega,\xi,\eta)\exp(\alpha x_1+\beta x_2)\times\phi_m(x_1,y_1)\phi_l(x_2,y_2)\,dx_2\,dy_2\,dx_1\,dy_1 \qquad (26)$$

$$M_{jm,\alpha}(t,\omega)=e^{-\alpha Ut}\int_0^t\exp[-(i\omega-\alpha U)\tau]h_{jm}(\tau)\,d\tau\times\int_0^{t-\tau}\dot{\psi}(\sigma)\exp[-(i\omega-\alpha U)\sigma]\,d\sigma$$

The cross-correlation function of the generalized responses ξ_j and ξ_k can now be expressed as

$$E[\xi_j(t_1)\xi_k(t_2)]=\int_{-\infty}^{\infty}\Psi_{jk}(t_1,t_2,\omega)\,e^{i\omega(t_1-t_2)}\,d\omega \qquad (19a)$$

where

$$\begin{aligned}\Psi_{jk}(t_1,t_2,\omega)=(\pi\rho_0U)^2{C_0}^2\sum_m\sum_l\\ [\Theta_{ml,\alpha\alpha}(\omega)M_{jm,\alpha}(t_1,\omega)M_{kl,\alpha}{}^*(t_2,\omega)-\\ \Theta_{ml,\alpha\beta}(\omega)M_{jm,\alpha}(t_1,\omega)M_{kl,\beta}{}^*(t_2,\omega)-\\ \Theta_{ml,\beta\alpha}(\omega)M_{jm,\beta}(t_1,\omega)M_{kl,\alpha}{}^*(t_2,\omega)+\\ \Theta_{ml,\beta\beta}(\omega)M_{jm,\beta}(t_1,\omega)M_{kl,\beta}{}^*(t_2,\omega)]\end{aligned} \qquad (27)$$

The quantity defined by Eq. (27) is the evolutionary cross spectral density function of the jth and kth generalized displacements at time instants t_1 and t_2, respectively. The mean square value of each modal response can be evaluated as the special case of $j=k$ and $t_1=t_2$, and by carrying out the integration in Eq. (19a). The correlation of the total response at (x_1,y_1) and (x_2,y_2) is given by

$$E[Z(x_1,y_1,t_1)Z(x_2,y_2,t_2)]=\sum_j\sum_k\phi_j(x_1,y_1)\phi_k(x_2,y_2)E[\xi_j(t_1)\xi_k(t_2)] \qquad (28)$$

The correlation of the derivatives of the modal responses can be obtained by

$$E[\xi_j{}^{(J)}(t_1)\xi_k{}^{(K)}(t_2)]=\partial^{J+K}E[\xi_j(t_1)\xi_k(t_2)]/\partial t_1{}^J\,\partial t_2{}^K \qquad (29)$$

provided that the right-hand side of Eq. (29) is bounded where J and K are non-negative integers and

$$\xi_j{}^{(J)}(t)=d^J\xi_j(t)/dt^J$$

Substitution of Eq. (19a) into Eq. (29) results in

$$E[\xi_j{}^{(J)}(t_1)\xi_k{}^{(K)}(t_2)]=\int_{-\infty}^{\infty}\Psi_{jk;J,K}(t_1,t_2,\omega)\,e^{i\omega(t_1-t_2)}\,d\omega \qquad (30)$$

where

$$\begin{aligned}\Psi_{jk;J,K}(t_1,t_2,\omega)=(\pi\rho_0U)^2{C_0}^2\sum_m\sum_l\\ [\Theta_{ml,\alpha\alpha}(\omega)\,{}_JM_{jm,\alpha}(t_1,\omega)\,{}_KM_{kl,\alpha}{}^*(t_2,\omega)-\\ \Theta_{ml,\alpha\beta}(\omega)\,{}_JM_{jm,\alpha}(t_1,\omega)\,{}_KM_{kl,\beta}{}^*(t_2,\omega)-\\ \Theta_{ml,\beta\alpha}(\omega)\,{}_JM_{jm,\beta}(t_1,\omega)\,{}_KM_{kl,\alpha}{}^*(t_2,\omega)+\\ \Theta_{ml,\beta\beta}(\omega)\,{}_JM_{jm,\beta}(t_1,\omega)\,{}_KM_{kl,\beta}{}^*(t_2,\omega)]\end{aligned} \qquad (31)$$

and

$${}_JM_{jm,\alpha}(t,\omega)=\sum_{I=0}^{J}\binom{J}{I}(i\omega)^I\,\partial^{J-I}M_{jm,\alpha}(t,\omega)/\partial t^{J-I} \qquad (32)$$

The function $\Psi_{jk;J,K}(t_1,t_2,\omega)$ has an even real part and an odd imaginary part with respect to ω. It is clear from Eq. (30) that when $t_1=t_2=t$ only the real part contributes to the integral. In the numerical example to be discussed later we shall be concerned particularly with the following quantities:

$$\Psi_{D,jk}(t,\omega)=\mathrm{Re}[\Psi_{jk;0,0}(t,t,\omega)]=\mathrm{Re}[\Psi_{jk}(t,t,\omega)] \qquad (33)$$

$$\Psi_{A,jk}(t,\omega)=\mathrm{Re}[\Psi_{jk;2,2}(t,t,\omega)] \qquad (34)$$

III. Response of an Airplane with a Swept-Back Wing

To illustrate the application of the analytical results derived in the preceding sections, we shall choose a rather simple configuration which, nevertheless, epitomizes the characteristics of a practical airplane. We consider here an idealized airplane with a swept-back wing, as shown in Fig. 1, a shape common for large, high-speed vehicles. The wing carries an attached mass which is distributed uniformly along the x axis over a length $2b$, and which does not contribute to the wing rigidity. The wing has a bending rigidity EI, and a mass distribution m per unit length in the $\bar{y}$ direction. Both EI and m are assumed to be constant. We shall assume that the wing bending mode shapes may be approximated by those of a cantilever beam with a skewed "effective root."[4]

The following three degrees-of-freedom will be considered:

plunging: $w_1(x,y)=1$

pitching: $w_2(x,y)=-x$

fundamental wing bending:

$$w_3(x,y)=S_1\,e^{-\Omega_3\bar{y}/l}+S_2\cos\Omega_3\bar{y}/l+S_3\sinh\Omega_3\bar{y}/l+S_4\sin\Omega_3\bar{y}/l \qquad (35)$$

where

$$\begin{aligned}\begin{Bmatrix}\bar{x}\\ \bar{y}\end{Bmatrix}&=\begin{bmatrix}\cos\Lambda & -\sin\Lambda\\ \sin\Lambda & \cos\Lambda\end{bmatrix}\begin{Bmatrix}x\\ y\end{Bmatrix} \quad \text{for} \quad y>0\\ &=\begin{bmatrix}\cos\Lambda & \sin\Lambda\\ -\sin\Lambda & \cos\Lambda\end{bmatrix}\begin{Bmatrix}x\\ y\end{Bmatrix} \quad \text{for} \quad y<0\end{aligned} \qquad (36)$$

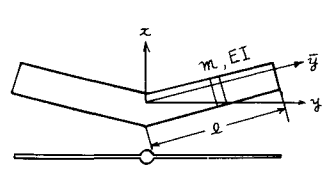

Fig. 1 An idealized model of an airplane.

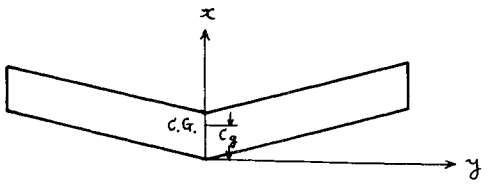

Fig. 2 New coordinate system.

and Λ is the sweep angle. Denote: m_F = distributed fuselage mass per unit length along x axis; ρ_w = distributed wing mass per unit area; $M_T = 2M_F + 2ml$ = the total mass; $M_F = bm_F$ = one-half of fuselage mass; $m = 2b\rho_w \cos\Lambda$ = wing mass per unit span; $R = M_F/ml$ = ratio of fuselage mass to wing mass. The coefficients S_1, S_2, S_3, S_4 and the constant Ω_3 in the expression for w_3 can be computed from the mass ratio R. The natural frequency corresponding to the fundamental wing bending mode is given by

$$\omega_3 = (\Omega_3/l)^2(EI/m)^{1/2} \tag{37}$$

and those of plunging and pitching rigid modes, ω_1 and ω_2, are known to be zero. The characteristic functions ϕ_i required for the computation of the generalized masses, generalized forces, etc., are obtained by normalizing the shape functions w_i; that is,

$$\phi_i(x, y) = N_i w_i(x, y) \tag{38}$$

where N_i is determined from

$$\int_S\int \rho(x, y)\phi_i^2(x, y)\, dx\, dy = M_T \tag{39}$$

For convenience of calculation, we shift the origin of the coordinates to the front tip of the wing (see Fig. 2). It can be shown that the distance c_g from the new origin to the gravity center is

$$c_g = b + [l \sin\Delta/2(R+1)] \tag{40}$$

We then calculate the geometrical coefficients and normalizing constants from Eq. (39) and from

$$\delta_{ij} = \int_S\int w_i(x - c_g, y)w_j(x - c_g, y)\, dx\, dy \tag{41}$$

$$\Delta_{ij} = N_i N_j \delta_{ij} \tag{42}$$

The constants Δ_{ij} are required for the computation of the following matrix which appears in the expression for the Laplace transforms of impulse response functions:

$$[C_{jm}] = \begin{bmatrix} M_1p^2 + \bar{f}(p)\Delta_{11} + \beta_1 p, & \bar{f}(p)\Delta_{12}, & \bar{f}(p)\Delta_{13} \\ \bar{f}(p)\Delta_{21}, & M_2p^2 + \bar{f}(p)\Delta_{22} + \beta_2 p, & \bar{f}(p)\Delta_{23} \\ \bar{f}(p)\Delta_{31}, & \bar{f}(p)\Delta_{32}, & M_3p^2 + M_3\omega_3^2 + \bar{f}(p)\Delta_{33} + \beta_3 p \end{bmatrix} \tag{43}$$

where $\bar{f}(p) = \pi\rho_0 U[p^2\bar{\phi}(p) + (b/2U)p^2]$ and $\bar{\phi}(p)$ is the Laplace transform of Wagner's function which is given by

$$\bar{\phi}(p) = \frac{1}{p} - \frac{0.165}{p + 0.0455U/b} - \frac{0.335}{p + 0.3U/b}$$

It can be shown that $\bar{f}(p)$ may be expressed as follows:

$$\bar{f}(p) = p(B_3p^3 + B_4p^2 + B_5p + B_6)/(p + B_1)(p + B_2) \tag{44}$$

where

$$A_1 = 0.5, \quad A_2 = 0.2807575(U/b), \quad A_3 = 0.01365(U/b)^2$$
$$B_1 = 0.0455(U/b), \; B_2 = 0.3(U/b), \; B_3 = \pi\rho_0(b/2)$$
$$B_4 = \pi\rho_0 U[A_1 + (B_1 + B_2)b/2U], \quad B_5 = \pi\rho_0 U[A_2 + B_1B_2b/2U]$$
$$B_6 = \pi\rho_0 UA_3$$

Then after a straightforward algebraic manipulation the Laplace transformation of impulse response function is reduced to the following form:

$$\bar{h}_{ij}(p) = \sum_{k=1}^{N(i,j)} E_{ij,k}p^{k-1} \Big/ p\sum_{l=1}^{11} H_l p^{l-1} \tag{45}$$

where

$$N(i,j) = \begin{cases} 10, & i = j \\ 9, & i \neq j \end{cases}$$

and $E_{ij,1} = 0$ when either $i = 3$, or $j = 3$, or both. The denominator in Eq. (45) is the determinant of matrix $[C_{jm}]$ and the numerator is the cofactor of the (i,j) element of this matrix.

Let the characteristic roots of matrix $[C_{jm}]$ be $\gamma_1, \gamma_2, \ldots, \gamma_{11}$ and let $\gamma_{11} = 0$. We obtain the following general form for the impulse response function:

$$h_{ij}(\tau) = \sum_{m=1}^{M(i,j)} A_{ij,m}\exp(\gamma_m\tau) \tag{46}$$

where

$$A_{ij,m} = \sum_{k=1}^{N(ij)} E_{ij,k}\gamma_m^{k-1} \Big/ \left[\frac{d}{dp}\left(p\sum_{l=1}^{11} H_l p^{l-1}\right)\right]_{p=\gamma_m}$$

and $M(i,j)$ is equal to 10 when either $i = 3$, or $j = 3$, or both, and for any other combinations $M(i,j) = 11$. From the symmetry of matrix $[C_{jm}]$, we see that§ $h_{ij}(\tau) = h_{ji}(\tau)$.

The roots $\gamma_1, \gamma_2, \ldots, \gamma_{10}$ are either real or in complex conjugate pairs. If γ_m and γ_{m+1} are a pair of conjugate roots, the corresponding coefficients $A_{ij,m}$ and $A_{ij,m+1}$ in Eq. (46) must also be a conjugate pair since the resulting sum must be real.

The impulse response function, Eq. (46), and the following derivative of Küssner's function

$$\dot{\psi}(\sigma) = (U/2b)\{0.13\exp[-0.13(U/b)\sigma] + \exp[-(U/b)\sigma]\}$$

can now be substituted into the second equation of (26) resulting in

$$M_{jm,z}(t,\omega) = \frac{U}{2b}\sum_{l=1}^{M(j,m)} A_{jm,l} \times$$
$$\left\{\left[\frac{0.13}{(-0.13U/b - i\omega + \alpha U)(0.13U/b + \gamma_l)} + \frac{1}{(-U/b - i\omega + \alpha U)(U/b + \gamma_l)} - \frac{0.13}{(-0.13U/b - i\omega + \alpha U)(-i\omega + \alpha U + \gamma_l)} - \frac{1}{(-U/b - i\omega + \alpha U)(-i\omega + \alpha U + \gamma_l)}\right] e^{(-i\omega+\gamma_l)t} - \right.$$
$$\frac{0.13}{(-0.13U/b - i\omega + \alpha U)(0.13U/b + \gamma_l)} e^{(-0.13U/b - i\omega)t} -$$
$$\frac{1}{(-U/b - i\omega + \alpha U)(U/b + \gamma_l)} e^{(-U/b - i\omega)t} +$$
$$\left.\left[\frac{0.13}{-0.13U/b - i\omega + \alpha U} + \frac{1}{-U/b - i\omega + \alpha U}\right]\frac{e^{-\alpha Ut}}{(-i\omega + \alpha U + \gamma_l)}\right\} \tag{47}$$

The computation of the function $\Theta_{mn,\alpha\beta}(\omega)$, the first equation of (26), involves the modified Bessel functions which appear in the expression for $\Phi(\omega, \xi, \eta)$, Eq. (21). To obtain some physical insight into an approximate expression for $\Phi(\omega, \xi, \eta)$ to be proposed later, let us consider first the following two limiting cases: the case of $L_G \to \infty$ and the case of $L_G \to 0$. As can be seen from Eq. (21), when L_G is very large, Φ decreases as $1/L_G$. Thus,

$$\lim_{L_G\to\infty} \Phi(\omega, \xi, \eta) = 0$$

This is reasonable since a forcing field with an infinite correlation length does not cause a disturbance to an airplane. On the other hand, when L_G is very small, we may use

$$\lim_{z\to\infty} zK_1(z) = 0 \qquad \lim_{z\to\infty} z^2K_2(z) = 0$$

in Eq. (21). Thus, we are led also to

$$\lim_{L_G\to 0} \Phi(\omega, \xi, \eta) = 0$$

§ This property may not hold true when more accurate aerodynamic forces are considered.

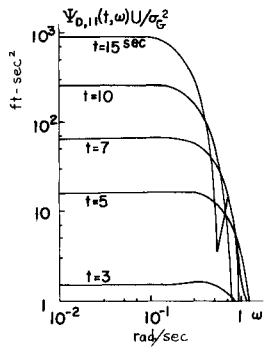

Fig. 3 Displacement evolutionary spectra—plunging mode.

Physically, this means that the effects of many minute uncorrelated disturbances on a large airplane tend to cancel each other. Therefore, an airplane does not respond to a turbulence field with either an extremely large or an extremely small turbulence scale. The same observation was previously made by Fung.[7] Actually, zero response for both $L_G \to 0$ and $L_G \to \infty$ comes from a zero input spectrum.

In most practical applications we are interested in those cases where L_G remains finite but

$$|\eta/L_G| \ll 1$$

Noting that as $z \to 0$,

$$zK_1(z) \to 1, \qquad z^2k_2(z) \to 2$$

we find that, for negligibly small $|\eta/L_G|$,

$$\Phi(\omega,\xi,\eta) \approx \Phi_d(\omega)\, e^{-i\omega\xi/U} \tag{48}$$

where

$$\Phi_d(\omega) = \frac{\sigma_G{}^2 L_G}{2\pi U} \frac{1+3(\omega L_G/U)^2}{[1+(\omega L_G/U)^2]^2}$$

This Φ_d function is known as Dryden's spectrum, and it has been used in a previous analysis where only the plunging motion was considered.[2] Of course, Φ would reduce to Φ_d if $\omega\xi/U$ were negligibly small. However, this further simplification would result in unacceptable errors especially in computing the wing bending response.

Substitution of Eq. (48) into the first equation in (26) yields

$$\Theta_{ml,\alpha\beta}(\omega) = \Phi_d(\omega) R_{m,\alpha} R_{l,\beta}{}^* \tag{49}$$

where

$$R_{m,\alpha} = e^{-\alpha c_g} \int_S \int \phi_m(x-c_g, y)\, e^{(\alpha - i\omega/U)x}\, dx\, dy \tag{50}$$

From straightforward integrations, we obtain

$$R_{1,\alpha} = 2\exp(-c_g\alpha)[\exp(2bA)-1][\exp(Al\sin\Lambda)-1]/(A^2\tan\Lambda)$$

$$R_{2,\alpha} = N_2 c_g R_{1,\alpha} - 2N_2\exp(-c_g\alpha)[(Al\sin\Lambda+2bA-2)\times \exp(2bA+Al\sin\Lambda)+2(1-bA)\exp(2bA)+ Al\sin\Lambda\exp(Al\sin\Lambda)-2]/(A^3\tan\Lambda)$$

$$R_{3,\alpha} = \exp(-c_g\alpha) I_{3,\alpha}$$

where

$$A = \alpha - i\omega/U$$

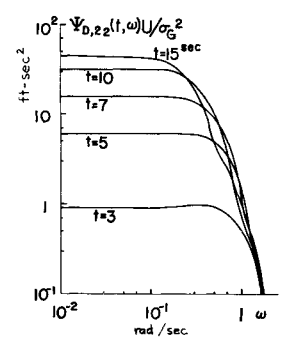

Fig. 4 Displacement evolutionary spectra—pitching mode.

Table 1 Physical data for numerical example

$l = 42$ ft	$R = 3$
$b = 7$ ft	$\Omega_3 = 1.955$
$\Lambda = 30°$	$L_G = 750$ ft
$U = 400$ m.p.h. (586.6 fps)	$\alpha = 0.1\times10^{-3}$ ft^{-1}
$EI = 1.2\times10^9$ lb-ft^2	$\beta = 0.4\times10^{-3}$ ft^{-1}
$\rho_w = 2.5$ slugs/ft^2	$\omega_3 = 13.63$ rad/sec

$$\tilde{\Omega}_3 = \Omega_3/l\cos\Lambda, \quad A_t = A\tan\Lambda$$

$$\Lambda_0 = \Omega_3\sin\Lambda(c_g/l)$$

$$\Lambda_1 = \Omega_3\sin\Lambda(2b-c_g)/l$$

$$\Pi_1 = N_3S_1[\exp(2bA+\Lambda_1)-\exp(-\Lambda_0)]/(A+\Omega_3\sin\Lambda/l)$$

$$\Pi_2 = N_3S_1[\exp(2bA-\Lambda_1)-\exp(\Lambda_0)]/(A-\Omega_3\sin\Lambda/l)$$

$$\tilde{C} = 2S_2[A\cos\Lambda_1+\Omega_3\sin\Lambda_1\sin\Lambda/l)\exp(2bA)- (A\cos\Lambda_0-\Omega_3\sin\Lambda_0\sin\Lambda/l)]N_3$$

$$\tilde{S} = 2S_2[(-A\sin\Lambda_1+\Omega_3\cos\Lambda_1\sin\Lambda/l)\exp(2bA)- (A\sin\Lambda_0+\Omega_3\cos\Lambda_0\sin\Lambda/l)]N_3$$

$$I_{3,\alpha} = \Pi_1[\exp(Al\sin\Lambda+\Omega_3)-1]/(A_t+\tilde{\Omega}_3)+ \Pi_2[\exp(Al\sin\Lambda-\Omega_3)-1]/(A_t-\tilde{\Omega}_3)+ \{[\tilde{C}(A\tan\Lambda\cos\Omega_3+\Omega_3\sin\Omega_3\sin\Lambda/l)+ \tilde{S}(A\tan\Lambda\sin\Omega_3-\Omega_3\cos\Omega_3\sin\Lambda/l)]\times \exp(Al\sin\Lambda)-\tilde{C}A\tan\Lambda+\tilde{S}\Omega_3\sin\Lambda/l\}/(A_t{}^2+\tilde{\Omega}_3{}^2)$$

IV. Numerical Examples

The physical data used for numerical calculation are given in Table 1. The structural damping is assumed to be zero.

The evolutionary spectral densities for the generalized displacements are shown in Figs. 3–5 for the plunging, pitching, and fundamental wing bending, respectively. The results for the plunging and pitching modes show a similar frequency distribution where high-level responses are found in the neighborhood around the zero frequency. The evolutionary spectral densities for fundamental wing bending depicted in Fig. 5 exhibit marked differences from those of the rigid modes. These curves show two dominant peaks, one around 1 rad/sec and another at the fundamental natural frequency for wing bending. Clearly, the first peak is due to the high energy content of the input in the low-frequency region and the second peak is due to the high transmittancy of energy near the first bending frequency. The spectral level tapers off very rapidly beyond this frequency.

The results for plunging and pitching acceleration shown in Figs. 6 and 7 again resemble each other, but their general trend with respect to frequency ω is quite different from the corresponding displacement spectra. As time increases, there is a gradual shift of spectral distribution from lower frequency to around frequency $\omega = 1$ rad/sec. The result for the bending mode acceleration shown in Fig. 8 exhibits only one peak at the fundamental natural frequency of the wing bending.

The evolutionary cross spectral densities for two different modes such as plunging-pitching, plunging-bending, etc. for both

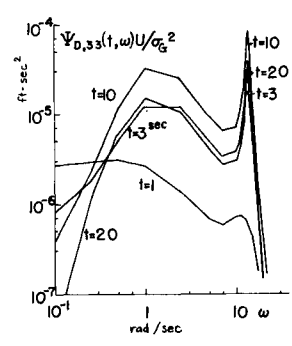

Fig. 5 Displacement evolutionary spectra—wing fundamental bending.

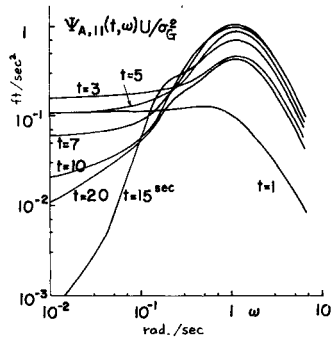

Fig. 6 Acceleration evolutionary spectra—plunging mode.

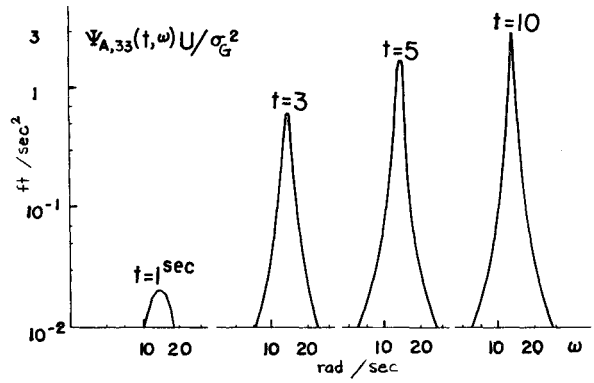

Fig. 8 Acceleration evolutionary spectra—wing fundamental bending.

displacement and acceleration response have also been computed but not graphically presented herein. These are generally complex-valued, and both the real part and the imaginary part may be either positive or negative at given t and ω. However, for the present numerical example, the absolute values of these evolutionary cross-spectra were found to be insignificant when compared with the evolutionary spectral densities shown in Figs. 3–8; therefore, their contribution to the total mean-square response is negligible.

Concluding Remarks

The primary purposes of the present paper are to derive the basic general formulas required for a nonstationary analysis of vehicle response to atmospheric turbulence when several degrees of freedom in the airplane motion are considered, and to demonstrate the feasibility of such an analysis. These objectives have been accomplished even though rather sweeping simplifications were made in regard to structural and aerodynamic characteristics, to avoid being bogged down with computational details. If the theory is to be used for practical designs then much more accurate evaluation of structural and aerodynamic parameters will be necessary. However, refinements along these lines should not be too difficult with modern high-speed digital computers. For example, the assumptions for uniform distribution of mass along the fuselage and along the wing span, for uniform wing bending stiffness, for the negligibility of wing torsion and the substitution of cantilever beam bending modes for swept wing bending modes are all oversimplifications, but with recent advancement in matrix methods of structural analysis and the availability of an electronic digital computer any configuration can be handled quite adequately. On the aerodynamics side, the vortex method for numerical computation of unsteady lift and the extension to the double-lattice method[8] can be applied to arbitrary lifting surfaces, including nonplanar ones.

Nevertheless, certain features in the results of the present simplified analysis, Figs. 3–8, are expected to remain unchanged when a more accurate account is taken of structural and aerodynamic parameters. Among these, we mention the high spectral levels in the very low-frequency region for rigid-body displacements, the presence of double peaks for the elastic displacement mode, and, in the case of acceleration responses, the energy shift from lower frequencies resulting in a single peak for both rigid and elastic modes.

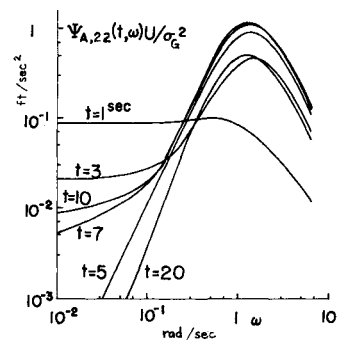

Fig. 7 Acceleration evolutionary spectra—pitching mode.

References

[1] Houbolt, J. C., Steiner, R., and Pratt, K. G., "Dynamic Response of Airplanes to Atmospheric Turbulence Including Flight Data on Input and Response," TR-199, 1964, NASA.

[2] Howell, L. J. and Lin, Y. K., "Response of Flight Vehicles to Nonstationary Random Atmospheric Turbulence," *AIAA Journal*, Vol. 9, No. 11, Nov. 1971, pp. 2201–2207.

[3] Priestley, M. B., "Evolutionary Spectra and Nonstationary Process," *Journal of the Royal Statistical Society*, Ser. B, Vol. 27, No. 2, 1965, pp. 204–228.

[4] Bisplinghoff, R. L., Ashley, H., and Halfman, R. L., *Aeroelasticity*, Addison Wesley, Reading, Mass., 1955.

[5] Lin, Y. K., *Probabilistic Theory of Structural Dynamics*, McGraw-Hill, New York, 1967.

[6] Shinozuka, M., "Random Processes with Evolutionary Power," *Proceedings of the American Society of Civil Engineering; Journal of Engineering Mechanics Division*, No. EM4, Aug. 1970, pp. 543–545.

[7] Fung, Y. C., "Statistical Aspect of Dynamic Load," *Journal of Aeronautical Sciences*, Vol. 20, May 1953, pp. 317–330.

[8] Kalman, T. P., Rodden, W. P., and Giesing, J. P., "Application of the Double-Lattice Method of Nonplanar Configurations in Subsonic Flow," *Journal of Aircraft*, Vol. 8, No. 6, June 1971, pp. 406–413.